Taylor & Francis
Taylor & Francis Group

Journal of Quality Technology

A Quarterly Journal of Methods, Applications and Related Topics

ISSN: 0022-4065 (Print) 2575-6230 (Online) Journal homepage: www.tandfonline.com/journals/ujqt20

A unified class of process capability indices for asymmetric tolerances and non-normal data

Shixiang Li, Sheng Fu, Dianpeng Wang & Piao Chen

To cite this article: Shixiang Li, Sheng Fu, Dianpeng Wang & Piao Chen (2025) A unified class of process capability indices for asymmetric tolerances and non-normal data, Journal of Quality Technology, 57:3, 200-219, DOI: 10.1080/00224065.2025.2497372

To link to this article: https://doi.org/10.1080/00224065.2025.2497372

JOURNAL OF QUALITY TECHNOLOGY
2025, VOL. 57, NO. 3, 200–219
https://doi.org/10.1080/00224065.2025.2497372

A unified class of process capability indices for asymmetric tolerances and non-normal data

Shixiang Li[a], Sheng Fu[b], Dianpeng Wang[c], and Piao Chen[d]

[a]Department of Applied Mathematics, Delft University of Technology, Delft, the Netherlands; [b]School of Statistics and Data Science, KLMDASR, LEBPS, and LPMC, Nankai University, Tianjin, China; [c]School of Mathematics and Statistics, Beijing Institute of Technology, Beijing, China; [d]ZJU-UIUC Institute, Zhejiang University, Haining, China

ABSTRACT

Process capability analysis plays a critical role in quality control by evaluating how well manufacturing processes meet defined specifications. However, traditional process capability indices (PCIs) rely on assumptions of symmetric tolerances and normally distributed data, which often do not hold in real-world applications and can lead to misleading conclusions. To overcome these limitations, we propose two novel classes of PCIs designed specifically for asymmetric tolerances, complemented by parametric estimation procedures and asymptotic confidence limits. To address the issue of non-normal data, we further employ an inverse transformation *via* constrained B-spline regression, which removes the need for the normality assumption. We demonstrate that our proposed PCIs reduce to traditional indices under symmetric conditions and normal data while extending applicability to a broader range of cases. Numerical simulations and a real-world application in an electronics company confirm the effectiveness and practical utility of our approach.

KEYWORDS

non-normal distribution; PCI; quality assurance; regression spline

1. Introduction

1.1. Background

Process capability refers to the capability of an in-control production process in manufacturing conforming products. For a given product, there are usually various requirements on its quality determined by customers' needs and/or engineering tolerances, and they are called specification limits. A capable production process should have the distribution of its quality characteristic lie almost completely within the specification limits. The process capability analysis has been performed by most manufacturing companies worldwide and its importance is significantly increasing due to the role of product quality in the modern competitive market.

In practice, process capability is often quantified by using process capability indices (PCIs) and they have been widely applied in a variety of industries to evaluate the machining process quantitatively (Otsuka and Nagata 2018; Tomohiro, Arizono, and Takemoto 2020; Wang, Chen, and Tan 2019; Wu, Pearn, and Kotz 2009). Consider a univariate quality characteristic X which is assumed to follow a normal distribution $N(\mu, \sigma^2)$. Let LSL and USL be the lower and upper specification limits, respectively. The earliest PCIs are C_p and C_{pk}, which are defined as

$$C_p = \frac{USL - LSL}{6\sigma}, \qquad C_{pk} = \min\left\{\frac{USL - \mu}{3\sigma}, \frac{\mu - LSL}{3\sigma}\right\}. \tag{1}$$

Generally speaking, C_p measures the spread of the distribution relative to the manufacturing tolerance as a measure of process precision, but it does not take the center of the distribution into account. This limitation is overcome in the construction of C_{pk}, where both the center and spread of the distribution are considered. On the other hand, customers may have an expectation of the quality characteristic of the products. To take the target value T into account, C_{pm} and C_{pmk} were further developed and they are given by

$$C_{pm} = \frac{C_p}{\sqrt{1 + \left(\frac{\mu - T}{\sigma}\right)^2}}, \qquad C_{pmk} = \frac{C_{pk}}{\sqrt{1 + \left(\frac{\mu - T}{\sigma}\right)^2}}. \tag{2}$$

CONTACT Piao Chen piaochen@intl.zju.edu.cn ZJU-UIUC Institute, Zhejiang University, Haining, China.

It is clear that these two PCIs are adapted from C_p and C_{pk} but they further reflect to which extent the process mean differs from the target value.

It is important to note that the above-mentioned classical PCIs rely on two assumptions. Firstly, the quality characteristic X is assumed to be normal. Although this assumption is widely adopted in the PCI literature, it may not be appropriate for a variety of quality characteristics (Kumar et al. 2022; Shaabani and Jafari 2024). Some examples include the measurements of metallic impurities in silicon wafers (Bittanti, Lovera, and Moiraghi 1998), the weights of rubber edges (Chen and Pearn 1997), and the capacitances of non-polarized capacitors (Pearn and Chen 1997). When the normality assumption is violated, the classical PCIs may lead to incorrect assessments (Momeni, Sadeghpour Gildeh, and Hesamian 2019). Secondly, the target value T is implicitly assumed to be in the middle point of the specification limits, i.e., $T = (USL + LSL)/2$. In the presence of asymmetric tolerances, C_{pm} and C_{pmk} will produce unsatisfactory results as they cannot reflect process performance relative to the process characteristic staying within the tolerances. The asymmetric tolerance is however not uncommon in real applications when customers have different preferences in the two directions from the target value (Erfanian and Sadeghpour Gildeh 2021; Khlil, Al-Khazraji, and Alabacy 2020). Moreover, asymmetric tolerance naturally arises when data transformation is performed to achieve approximate normality.

There have been a variety of PCIs proposed in the literature to deal with the non-normal data and asymmetric tolerances, but few studies have considered these two important issues simultaneously. In the next subsection, we give a literature review of the existing PCIs.

1.2. Literature review

For the purpose of concise presentation, we first introduce the following superstructure proposed by Vännman (1995) which unifies the four classical PCIs

$$C_p(u,v) = \frac{d - u|\mu - M|}{3\sqrt{\sigma^2 + v(\mu - T)^2}}, \qquad [3]$$

where $u, v \geq 0, d = (USL - LSL)/2$, and $M = (USL + LSL)/2$. It is easy to see that $C_p(0,0) = C_p$, $C_p(1,0) = C_{pk}, C_p(0,1) = C_{pm}$, and $C_p(1,1) = C_{pmk}$. In the following two subsections, we review the existing PCIs for asymmetric tolerances and non-normal process data, respectively.

1.2.1. PCIs for asymmetric tolerances

Adjusting asymmetric specification limits and then using classical PCIs on the new specification limits is one of the earliest ways to deal with asymmetric tolerances. Kane (1986) considered shifting one of the two specification limits and applied $(T - d^*, T + d^*)$ instead of the true limits $(T - D_l, T + D_u)$, where $D_l = T - LSL$, $D_u = USL - T$ and $d^* = \min\{D_l, D_u\}$. The PCIs can then be obtained by replacing d by d^* in the superstructure Eq. [3]. On the other hand, Franklin and Wasserman (1992) and Kushler and Hurley (1992) adjusted both limits in Eq. [3] to obtain the PCIs. By confining the process to a subset of the real specification range, these indices provide an approximate quantification of the process capability. However, depending on the location of μ relative to T, those PCIs either overstate or understate the true process capability.

The other category of methods is to propose tailored PCIs to address the asymmetric tolerances (Abbasi Ganji and Sadeghpour Gildeh 2016; Boyles 1994; Chen and Pearn 2001; Grau 2005; Wu et al. 2010; Vännman 1997). For example, Vännman (1997) considered the effects of the direction between μ and T, and proposed the PCIs by adding the term $|\mu - T|$ to the numerator of Eq. [3]. Because the so-obtained PCIs cannot reach the maximum at $\mu = T$ and occasionally yield negative values, Chen and Pearn (2001) further proposed another class of PCIs as

$$C_p^F(u,v) = \frac{d^* - uF^*}{3\sqrt{\sigma^2 + vF^2}}, \qquad [4]$$

where

$$F = \max\left\{\frac{d(\mu - T)}{D_u}, \frac{d(T - \mu)}{D_l}\right\},$$
$$F^* = \max\left\{\frac{d^*(\mu - T)}{D_u}, \frac{d^*(T - \mu)}{D_l}\right\}. \qquad [5]$$

This superstructure obtains its maximum at $\mu = T$ and is not symmetric around T, which reflects the customers' preference toward different directions from the target value. More recently, Abbasi Ganji and Sadeghpour Gildeh (2016) improved Eq. [4] by noting that $C_p^F(u,v)$ is zero at both specification limits, which may not be reasonable as PCIs at the closer limit to T should have a higher value. Toward this end, the authors replaced F^* by

$$A^* = \frac{(\mu - T)^2}{D_u} I\{\mu > T\} + \frac{(T - \mu)^2}{D_l} I\{\mu \leq T\}, \qquad [6]$$

and F by

$$A = \frac{d(\mu - T)}{D_u} I\{\mu > T\} + \frac{d(T - \mu)}{D_l} I\{\mu \le T\}. \quad [7]$$

To the best of our knowledge, these PCIs are by far the most sensitive to the departure of the process mean from the target value.

1.2.2. PCIs for non-normal data

There are broadly two approaches to developing PCIs when the quality characteristic is not normally distributed. The first approach is the percentile-based PCIs, originally proposed by Clements (1989). The core idea is to replace the traditional parameters μ and σ with distribution percentiles after fitting the data to a suitable probability distribution. Subsequent research has expanded this framework in multiple directions. For instance, Senvar and Kahraman (2014) enhanced its applicability by incorporating fuzzy sets to better handle data uncertainty and imprecision. Additionally, adaptations to specific probability distributions, such as the Rayleigh (Dariae and Sadeghpour Gildeh 2017), gamma (de Almeida et al. 2021), logistic-exponential (Dey et al. 2023), and inverse Gaussian (Guo et al. 2023), have further improved its flexibility and accuracy within defined distribution families. Furthermore, recent studies have emphasized the construction of confidence limits for percentile-based PCIs, contributing to their robustness and reliability (Kashif et al. 2023; Wang and Chen 2020; Wang et al. 2021). Despite these advancements, the effectiveness of this approach remains contingent on the accurate selection and estimation of an appropriate distribution, which can be challenging in practical applications.

The second approach is the data-transformation method, which has gained increasing attention in recent years as an alternative to the percentile-based approach. Instead of fitting the data to a specific distribution, this method transforms the original data into a normally distributed form, allowing existing PCIs to be directly applied. Commonly used transformations include the logarithmic transformation (Rosas Rivera, Hubele, and Lawrence 1995; West 2022), the Box-Cox transformation (Riani, Atkinson, and Corbellini 2023; Tang and Than 1999), and the inverse normal transformation (Wang, Yang, and Hao 2016; Zou et al. 2024). However, a key challenge of this approach is the difficulty in interpreting the results in the original data scale. To address this issue, Chen, Wang, and Ye (2019) proposed a transformation based on the cumulative distribution function (CDF), and demonstrates its applicability to any continuous process data while preserving a quantitative interpretation of process capability.

1.3. Aims and outline

Despite extensive research on PCIs, a unified and versatile framework that accommodates both different tolerance structures (symmetric or asymmetric) and data distributions (normal or non-normal) remains lacking. In particular, existing PCIs for asymmetric tolerances often lack key desirable properties, while kernel estimation methods for the inverse transformation in non-normal data are prone to substantial bias near the boundaries of the data range. To address these shortcomings, this study proposes new capability indices together with a novel inverse transformation method based on constrained B-spline regression. This approach not only resolves the limitations in handling asymmetric tolerances but also offers a more robust solution for non-normal data. Importantly, our unified framework remains applicable even when tolerances are symmetric and data are normally distributed, ensuring consistent performance across various settings. Consequently, it simplifies decision-making and enhances process capability assessment in a wide range of manufacturing scenarios.

The rest of this paper is organized as follows. In Section 2, we first give an in-depth discussion on the desirable properties of PCIs for the asymmetric tolerances, based on which two novel superstructures are proposed. Moreover, their relationships with the process centering and with the process yield are established. Section 3 provides comparison studies between the proposed PCIs and the existing ones through extensive simulations. Building on the idea of inverse CDF transforming, the non-normal issue is considered in Section 4. We propose a constrained B-spline regression model to obtain a smooth and non-decreasing estimator of the CDF and compare it with some existing methods. A real example is used for illustration in Section 5 and concluding remarks are given in Section 6.

2. New PCIs for asymmetric tolerances

In this section, we first give a thorough analysis of the existing PCIs for asymmetric tolerances and elucidate the essential properties that effective PCIs should embody. Subsequently, we introduce two innovative PCIs that encompass all discernible properties identified during our analysis. Throughout this section, we

assume that the quality characteristic X follows a normal distribution $N(\mu, \sigma^2)$.

2.1. Existing PCIs for asymmetric tolerances

As reviewed in Section 1.2, two useful PCIs for asymmetric tolerances were developed in Chen and Pearn (2001) and Abbasi Ganji and Sadeghpour Gildeh (2016), and their motivation is based on two deficiencies of the existing PCIs: 1). They are not maximized at $\mu = T$, which is undesirable because the PCIs give contradictory conclusions between process centering and process yield in such cases; 2). They do not reflect the directions of μ toward T and hence cannot reflect the customers' preferences. As an illustration, Figure 1 shows how these two PCIs change with μ when $(LSL,\ T,\ USL)$ are set as (8, 9.5, 13), $\sigma = 1$ and $u = v = 1$. As seen, both PCIs are maximized at $\mu = T$ and they are not symmetric about T.

One major problem with C_p^F, as noted by Abbasi Ganji and Sadeghpour Gildeh (2016), is that it does not credibly quantify the shifts from the target value. Take Figure 1 as an example, the PCI at LSL should be larger than the PCI at USL since T is closer to LSL and the process has the same yield at $\mu = USL$ and $\mu = LSL$. This deficiency is remedied by C_p^A, which yields different values at USL and LSL. However, C_p^A will be negative for a certain range of μ, which brings difficulty in interpreting the process yield. Moreover, unlike other PCIs, C_p^A does not degenerate to the classical PCIs when the process is symmetric, i.e., $T = M$, which further restricts its applications in practice.

Based on the above discussion, we summarize the describable properties of PCIs in the presence of asymmetric processes as follows.

i. PCIs should be maximized at $\mu = T$.
ii. PCIs should decline more steeply as μ shifts from T to the closer specification limit.
iii. PCIs should be smaller on the further specification limit to T than those on the closer specification limit.
iv. PCIs should be non-negative.
v. PCIs should degenerate to the classical ones when the tolerance is symmetric.

Table 1 summarizes the existing PCIs for asymmetric tolerance and their properties. As seen, none of them satisfies all the five properties, which motivates us to propose new PCIs.

2.2. Proposal I: $C_{pn1}(u, v)$

From Table 1, we can see that $C_p^F(u, v)$ meets all the desired properties except for the third one. Based on

Table 1. Summary of existing PCIs for asymmetric tolerances; x denotes violation of a certain property.

PCIs	(i)	(ii)	(iii)	(iv)	(v)
Kane (1986)	x	x	x		
Franklin and Wasserman (1992)	x	x	x		
Boyles (1994)		x	x	x	
Vännman (1997)	x	x	x		
Chen and Pearn (2001)			x		
Grau (2005)			x		
Wu et al. 2010			x		
Abbasi Ganji and Sadeghpour Gildeh (2016)				x	x

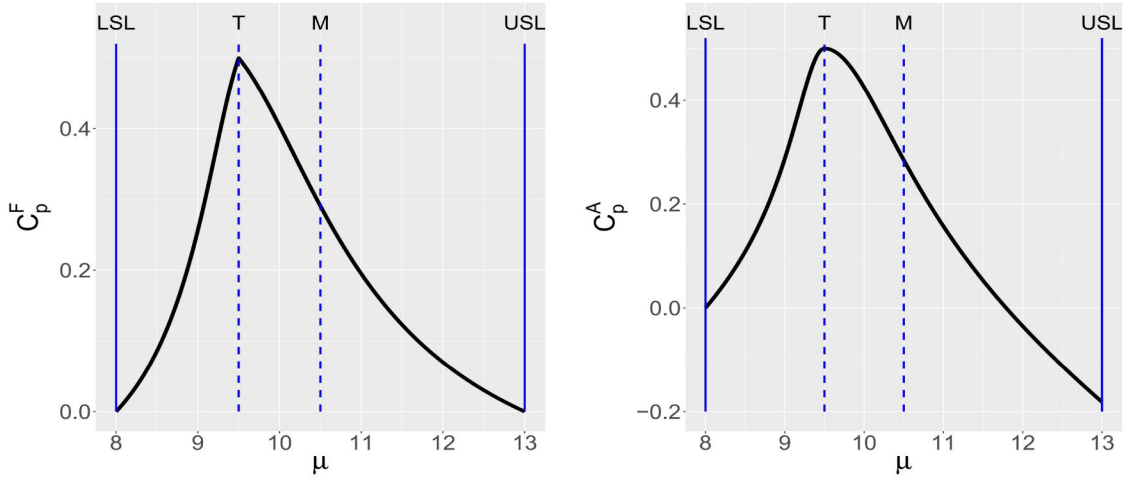

(a) Values of C_p^F for different μ.

(b) Values of C_p^A for different μ.

Figure 1. C_p^F, C_p^A values with $\sigma = 1$, $T = 9.5$ and μ ranging between the specification limits (8, 13).

the formula of $C_p^F(u,v)$ in Eq. [4], it is readily seen that F^* is equal to d^* when $u=1$ and $\mu = LSL$ or USL, making $C_p^F(1,v)=0$ at both specification limits. To make Property (iii) hold, we add an additional term $d^+ = \max\{D_l, D_u\}$ to the denominator of F^*, and the corresponding PCIs are now

$$C_{pn1}(u,v) = \frac{d^* - uF^+}{3\sqrt{\sigma^2 + vF^2}}, \tag{8}$$

where

$$\begin{aligned} F &= \max\left\{\frac{d(\mu - T)}{D_u}, \frac{d(T-\mu)}{D_l}\right\}, \\ F^+ &= \max\left\{\frac{2d^*(\mu - T)}{d^+ + D_u}, \frac{2d^*(T-\mu)}{d^+ + D_l}\right\}. \end{aligned} \tag{9}$$

Because F and F^+ are always non-negative, $C_{pn1}(u,v)$ reaches its maximum when $F = F^+ = 0$, which corresponds to the case of $\mu = T$. Secondly, by retaining D_l and D_u in F^+, Property (ii) holds for $C_{pn1}(u,v)$ when $u,\ v > 0$. Thirdly, F^+ is equal to d^* on the further limit and it is less than d^* on the closer limit. As a result, $C_{pn1}(u,v)$ remains 0 on the further limit and is strictly positive on the closer limit, which makes Property (iii) hold. Based on the above discussion, Property (iv) also holds for $C_{pn1}(u,v)$ when $0 \le u \le 1$. Lastly, we have $D_l = D_u = d^* = d^+ = d$ and $\max\{\mu - M, M - \mu\} = |\mu - M|$ when $T = M$. Therefore, $C_{pn1}(u,v)$ degenerates to the classical superstructure $C_p(u,v)$ in Eq. [3]. In summary, $C_{pn1}(u,v)$ meets all the five properties for any $u \in [0,1]$, $v \ge 0$.

2.2.1. Relation to process centering

Process centering is the ability of processes to congregate around the target value T, which can be measured as the distance between μ and T, i.e., $|\mu - T|$. For the tailored PCIs for asymmetric tolerances, it is important to link them with the process centering. Given $C_{pn1}(u,v) = c$, where c is often determined by engineers or customers in their purchasing contract, it is readily seen that

$$c = \frac{d^* - uF^+}{3\sqrt{\sigma^2 + vF^2}} \le \frac{d^* - uF^+}{3\sqrt{vF^2}}. \tag{10}$$

When $\mu > T$, we have

$$c \le \frac{d^* - u\frac{2d^*}{d^+ + D_u}(\mu - T)}{3\sqrt{v}\frac{d}{D_u}(\mu - T)}, \tag{11}$$

and hence

$$\mu - T \le \frac{d^*}{3c\sqrt{v}\frac{d}{D_u} + u\frac{2d^*}{d^+ + D_u}} \triangleq \lambda_1. \tag{12}$$

Similarly, when $\mu \le T$, we have

$$T - \mu \le \frac{d^*}{3c\sqrt{v}\frac{d}{D_l} + u\frac{2d^*}{d^+ + D_l}} \triangleq \lambda_1'. \tag{13}$$

Thus, the mean is bounded by

$$T - \lambda_1' \le \mu \le T + \lambda_1. \tag{14}$$

Note that we assume that $u \ne 0$ in the derivations, which is also adopted in Abbasi Ganji and Sadeghpour Gildeh (2016).

2.2.2. Relation to process yield

Another major role of PCIs is to infer the process yield, which is defined as the percentage of products that pass inspections, i.e., the probability of the quality characteristic that is within the specification limits. In practice, the process yield is often quantified by using the percentage of the non-conforming (NC) products, which is given by $\mathrm{NC} = P(X < LSL) + P(X > USL)$. We aim to build the relation between $C_{pn1}(u,v)$ and NC here.

Recall that $T - \lambda_1' \le \mu \le T + \lambda_1$. If the target is closer to the upper limit (i.e., $T > M$), we have more non-conforming products when $\mu > T$. Therefore, given $C_{pn1}(u,v) = c$, we have

$$\begin{aligned} \mathrm{NC} \le 2P(X > USL) &= 2[1 - P(X < USL)], \\ &= 2\left[1 - \Phi\left(\frac{USL - \mu}{\sigma}\right)\right], \\ &\le 2\left[1 - \Phi\left(\frac{D_u - \lambda_1}{\sigma}\right)\right]. \end{aligned} \tag{15}$$

From Eq. [10], we have $c \le \frac{d^*}{3\sigma}$, and hence σ is bounded by $\frac{d^*}{3c}$. As a result, the upper bound of NC is

$$\mathrm{NC} \le 2\left[1 - \Phi\left(\frac{3c(D_u - \lambda_1)}{d^*}\right)\right]. \tag{16}$$

Similarly, if the target is closer to the lower limit, i.e., $T \le M$, then we have more non-conforming products when $\mu \le T$. In such cases,

$$\begin{aligned} \mathrm{NC} \le 2P(X < LSL) &= 2\left[\Phi\left(\frac{LSL - \mu}{\sigma}\right)\right], \\ &= 2\left[1 - \Phi\left(\frac{\mu - LSL}{\sigma}\right)\right], \\ &\le 2\left[1 - \Phi\left(\frac{3c(D_l - \lambda_1')}{d^*}\right)\right]. \end{aligned} \tag{17}$$

2.3. Proposal II: $C_{pn2}(u, v)$

Our second proposal of the PCIs for asymmetric tolerances is based on the classical superstructure Eq. [3]. The major difficulty of the construction lies in Property (ii). To make the PCIs asymmetric about T, we introduce a ratio $R_1 = \min\{T/\mu,\ \mu/T\}$ as a function of μ. It is easy to check that $R_1(T+\epsilon)$ is larger than $R_1(T-\epsilon)$ for any $\epsilon > 0$. Therefore, R_1 is asymmetric about T and it is suitable for the case of $T < M$. Moreover, to make PCIs different at the two specification limits, another ratio function $R_2 = D_l/D_u$ is further introduced. Taken together, the second proposal $C_{pn2}(u, v)$ for $T < M$ is constructed as

$$C_{pn2}(u,v) = \frac{D_l - uR_2|\mu - T|}{3\sqrt{\sigma^2 + v(\mu - T)^2}} \times \mathcal{I}, \qquad [18]$$

where $\mathcal{I} = I\{T < M\} \times R_1 + I\{T = M\}$ and I is the indicator function. When $T > M$, given the sample $X_1, ..., X_n$ with the specification tolerances $(LSL,\ T,\ USL)$, we can apply the transformation $L - X_1, ..., L - X_n$ with a constant $L > \max\{X_1, ..., X_n\}$. Then, the transformed target value and middle point satisfies $L - T < L - M$, making Eq. [18] applicable. Without loss of generality, we only consider the case of $T < M$ for $C_{pn2}(u, v)$ in this study.

It remains to verify that C_{pn2} satisfies Property (i), (iv) and (v). Firstly, when $\mu = T$, R_2 is a constant and R_1 reaches its maximal value. Thus, C_{pn2} is maximized at $\mu = T$. Secondly, D_l is always larger than R_2 with $u \le 1$, and $\mathcal{I}$ is always positive. As a result, C_{pn2} is always non-negative. Lastly, when $T = M$, we have $D_l = D_u = d$, $R_2 = 1$ and $\mathcal{I} = 1$, and hence C_{pn2} degenerates to Eq. [3].

2.3.1. Relation to process centering

Given $C_{pn2}(u, v) = c$ and $T < M$, we have

$$c \le \frac{D_l - u\frac{D_l}{D_u} \times |\mu - T|}{3\sqrt{\sigma^2 + v(\mu - T)^2}} \times \frac{T}{\mu} \le \frac{D_l - u\frac{D_l}{D_u} \times |\mu - T|}{3\sqrt{v(\mu - T)^2}}, \qquad [19]$$

which indicates that

$$|\mu - T| \le \frac{D_l}{u\frac{D_l}{D_u} + 3c\sqrt{v}}. \qquad [20]$$

Therefore, the range of μ is symmetric about T, which is

$$T - \frac{D_l}{u\frac{D_l}{D_u} + 3c\sqrt{v}} \le \mu \le T + \frac{D_l}{u\frac{D_l}{D_u} + 3c\sqrt{v}}. \qquad [21]$$

Based on the derivation in Section 2.2.1, the range of μ given $C_{pn1} = c$ and $T < M$ is

$$T - \frac{D_l}{3c\sqrt{v}\frac{d}{D_l} + u\frac{2D_l}{D_u + D_l}} \le \mu \le T + \frac{D_l}{3c\sqrt{v}\frac{d}{D_u} + u\frac{D_l}{D_u}}. \qquad [22]$$

Because $d/D_u < 1$, the upper bound of μ based on C_{pn2} is smaller than that based on C_{pn1}. On the other hand, C_{pn1} gives tighter lower bound than C_{pn2} as $2D_l/(D_u + D_l) > D_l/D_u$ and $d/D_l > 1$. The detailed comparison is given in Section 2.4.

2.3.2. Relation to process yield

Similar to C_{pn1}, we can also derive the relation between C_{pn2} and NC. Under the assumption of normal distributions and $T < M$, we have

$$\begin{aligned} \mathrm{NC} \le 2P(X < LSL) &= 2\left[\Phi\left(\frac{LSL - \mu}{\sigma}\right)\right], \\ &= 2\left[1 - \Phi\left(\frac{\mu - LSL}{\sigma}\right)\right]. \end{aligned} \qquad [23]$$

Based on the lower bounds of μ in Eq. [21] and the similar upper bound of σ as in C_{pn1}, we have

$$\mathrm{NC} \le 2\left[1 - \Phi\left(3c\left(1 - \frac{D_u}{uD_l + 3D_u c\sqrt{v}}\right)\right)\right]. \qquad [24]$$

Compared with Eq. [17], this upper bound on NC is more conservative as the lower bound of μ based on C_{pn2} tends to be smaller.

2.4. Comparison studies

In this subsection, we demonstrate the properties of the two proposed PCIs by comparing them with C_p^F and C_p^A. We use the same settings as in Section 2.1, i.e., $(LSL,\ T,\ USL) = (8,\ 9.5,\ 13)$ and $\sigma = 1$. Figure 2 shows how the four PCIs vary when $\mu \in [8, 13]$ at $(u, v) = (0, 0), (0, 1), (1, 0)$ and $(1, 1)$. When $(u, v) = (0, 0)$, it is observed that C_{pn1}, C_p^F and C_p^A are the same constant because they all reduce to $d^*/(3\sigma)$, which does not depend on μ. This is undesirable because the difference between T and μ cannot be reflected. On the other hand, because of the term $\mathcal{I}$, C_{pn2} is able to take the direction of the departure from the target into account and it is maximized at $\mu = T$. Therefore, C_{pn2} is the only suitable PCI for asymmetric tolerances when $u = v = 0$.

Under the other three settings of (u, v), the four PCIs are all maximized at $\mu = T$ and asymmetric around T. Because of the intimate relation between C_{pn1} and C_p^F, it is not surprising to find that they

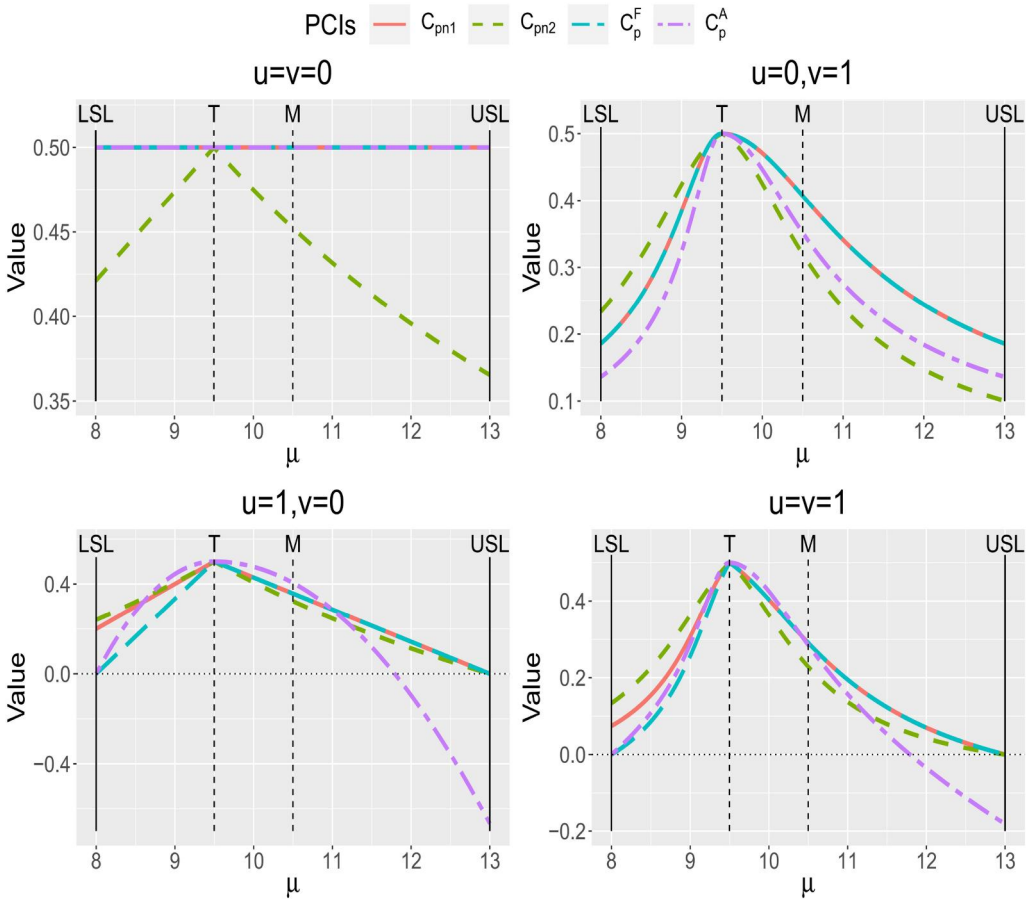

Figure 2. Numerical comparisons of C_{pn1}, C_{pn2}, C_p^F and C_p^A under different combinations of u and v, where $(LSL,\ T,\ USL) = (8,\ 9.5,\ 13)$ and $\sigma = 1$.

perform similarly in all the cases. In fact, they are identical when $\mu > T$, but C_{pn1} improves C_p^F by imposing the positive value at $\mu = LSL$ as T is closer to LSL than to USL. It is worth mentioning that C_p^A is also able to reflect the differences at the two specification limits, but it is the only one that yields negative values, violating Property (iv).

We then compare these four PCIs in terms of their relations with process centering and process yield. Because the bounds based on C_p^A are not well defined when $u = 0$ (Abbasi Ganji and Sadeghpour Gildeh 2016) and the bounds based on C_{pn1} and C_{pn2} are invariant to index values when $v = 0$, we only consider the case $(u, v) = (1, 1)$ here. Figure 3 shows the bounds of μ and NC given different PCIs when $u = v = 1$. As seen from the left panel, the trends of the bounds from all four PCIs are consistent: both the upper and lower bounds get tight first and then become loose, and the smallest gap is achieved when $\mu = T$ as the PCIs are maximized at $\mu = T$. Among the four PCIs, the lower bound based on C_{pn2} seems to be the most conservative but the upper bound is the tightest. On the other hand, C_{pn1} performs more similarly as C_p^F and C_p^A. Notably, the bounds based on C_p^A fail to contain the true mean when μ is large. This is because C_p^A becomes negative at large μ (see Figure 2), which further indicates the importance of Property (iv). On the other hand, the upper bounds of NC are conservative based on all the considered PCIs. Between the proposed C_{pn1} and C_{pn2}, C_{pn1} performs better and it is comparable to C_p^F. The bound based on C_p^A again has an irregular trend when μ is large because of the negative values of C_p^A.

Our comparative analysis demonstrates that the proposed C_{pn1} and C_{pn2} effectively address the limitations of C_p^F and C_p^A. Both indices evaluate whether manufactured items meet asymmetric specifications by credibly capturing process variability, yet they exhibit distinct behaviors—particularly in terms of process centering and yield. As highlighted by Ryan (2011), selecting an appropriate PCI is crucial in process capability studies. To guide this selection, we provide practical recommendations based on specific scenarios. For instance, as shown in Figure 2, C_{pn2} yields higher values when μ is closer to the LSL, thus offering a more conservative overall assessment. Consequently, C_{pn2} is recommended

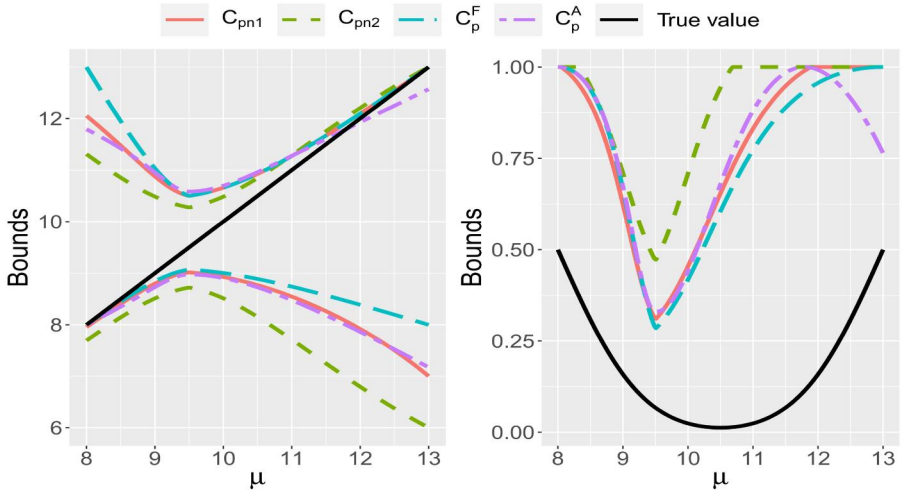

Figure 3. Upper and lower bounds of μ (left) and upper bounds of NC (right) given different PCIs. $LSL = 8$, $USL = 13$, $T = 9.5$, $\sigma = 1$ and $u = v = 1$.

when asymmetric tolerances exist and the cost implications of deviations in either direction are similar; it is also the sole meaningful index when $u = v = 0$. Conversely, if the primary concern is process centering and yield, C_{pn1} is preferable. In summary, the two proposed PCIs are designed for different application contexts, which provide a comprehensive and flexible framework for assessing process capability across diverse manufacturing scenarios.

3. Statistical inference

In practice, the proposed PCIs have to be estimated based on the observed data. Let $\boldsymbol{x} = [x_1, ..., x_n]^\top$ be a vector of random copies of the quality characteristic X. This section proposes point and interval estimation procedures for C_{pn1} and C_{pn2}.

3.1. Maximum likelihood estimation

Recall that $X \sim N(\mu, \sigma^2)$. The maximum likelihood (ML) estimators of μ and σ are $\hat{\mu} = \bar{x} \equiv \sum_{i=1}^n x_i/n$ and $\hat{\sigma}^2 = \sum_{i=1}^n (x_i - \bar{x})^2/n$. Based on the invariance property of ML estimators, the point estimators of C_{pn1} and C_{pn2} are

$$\begin{aligned} \hat{C}_{pn1}(u,v) &= \frac{d^* - u\hat{F}^+}{3\sqrt{\hat{\sigma}^2 + v\hat{F}^2}}, \\ \hat{C}_{pn2}(u,v) &= \frac{D_l - uR_2|\hat{\mu} - T|}{3\sqrt{\hat{\sigma}^2 + v(\hat{\mu} - T)^2}} \times \hat{\mathcal{I}}, \end{aligned} \tag{25}$$

where

$$\begin{aligned} \hat{F} &= \max\left\{\frac{d(\hat{\mu} - T)}{D_u}, \frac{d(T - \hat{\mu})}{D_l}\right\}, \\ \hat{F}^+ &= \max\left\{\frac{2d^*(\hat{\mu} - T)}{d^+ + D_u}, \frac{2d^*(T - \hat{\mu})}{d^+ + D_l}\right\}, \end{aligned} \tag{26}$$

$\widehat{R}_1 = \min\{T/\hat{\mu}, \hat{\mu}/T\}$, $R_2 = D_l/D_u$, and $\hat{\mathcal{I}} = I\{T < M\} \times \widehat{R}_1 + I\{T = M\}$.

On the other hand, the confidence limits of the PCIs are often of more interest in practice. There have been a multitude of studies addressing interval estimation in the literature (Cui, Yang, and Huang 2018; Ouyang, Dey, and Park 2024; Parchami and Mashinchi 2007), but few studies have investigated PCIs for asymmetric tolerances. Because of the complex forms in Eq. [25], the exact variance of $\hat{C}_{pn1}(u,v)$ and $\hat{C}_{pn2}(u,v)$ cannot be analytically derived. However, their asymptotic variance can be readily obtained by using the asymptotic variance of $\hat{\mu}$ and $\hat{\sigma}^2$. Note that $\sqrt{n}(\hat{\mu} - \mu) \xrightarrow{d} N(0, \sigma^2)$ and $\sqrt{n}(\hat{\sigma}^2 - \sigma^2) \xrightarrow{d} N(0, 2\sigma^4)$, where $\xrightarrow{d}$ denotes convergence in distribution. Given a function $g(x,y)$ with continuous first partial derivatives, the delta method yields that (Oehlert 1992)

$$\sqrt{n}\left[g(\bar{x}, \hat{\sigma}^2) - g(\mu, \sigma^2)\right] \xrightarrow{d} N(0, \nabla g(\mu,\ \sigma^2)\Sigma(\nabla g(\mu,\ \sigma^2))^\top), \tag{27}$$

where

$$\Sigma = \begin{pmatrix} \sigma^2 & 0 \\ 0 & 2\sigma^4 \end{pmatrix} \text{ and } \nabla g(x,y) = \left(\frac{\partial g}{\partial x}, \frac{\partial g}{\partial y}\right). \tag{28}$$

In terms of the proposed PCIs, we focus on the $T < M$ case and confidence limits for the $T > M$ case can be constructed in a similar way. In order to meet

the conditions on the derivatives, we derive the function $g_1(x,y)$ for $C_{pn1}(u,v)$ and $g_2(x,y)$ for $C_{pn2}(u,v)$ by considering three cases: $x > T$, $x = T$ and $x < T$. More specifically, we have

$$g_1(x,y) = \begin{cases} g_{11}(x,y) = \dfrac{D_l - u\frac{2d^*(x-T)}{d^+ + D_u}}{3\sqrt{y + v(\frac{d}{D_u}(x-T))^2}} & x > T, \\ g_{12}(x,y) = \dfrac{D_l}{3\sqrt{y}} & x = T, \\ g_{13}(x,y) = \dfrac{D_l - u\frac{2d^*(T-x)}{d^+ + D_l}}{3\sqrt{y + v(\frac{d}{D_l}(T-x))^2}} & x < T, \end{cases} \quad [29]$$

and

$$g_2(x,y) = \begin{cases} g_{21}(x,y) = \dfrac{D_l - u\frac{D_l}{D_u}(x-T)}{3\sqrt{y + v(x-T)^2}} \times \dfrac{T}{x} & x > T, \\ g_{22}(x,y) = \dfrac{D_l}{3\sqrt{y}} & x = T, \\ g_{23}(x,y) = \dfrac{D_l - u\frac{D_l}{D_u}(T-x)}{3\sqrt{y + v(x-T)^2}} \times \dfrac{x}{T} & x < T. \end{cases} \quad [30]$$

The delta method can then be invoked in each scenario, and the unknown parameters can be replaced by their ML estimators. In summary, the asymptotic variance of $C_{pni}(u,v)$, $i = 1, 2$, can be consistently estimated by

$$\hat{V}_i = \begin{cases} \nabla g_{i1}(\hat{\mu}, \hat{\sigma}^2)\hat{\Sigma}(\nabla g_{i1}(\hat{\mu}, \hat{\sigma}^2))^\top & \hat{\mu} > T, \\ \dfrac{\hat{D}_l^2}{18\hat{\sigma}^2} & \hat{\mu} = T, \\ \nabla g_{i3}(\hat{\mu}, \hat{\sigma}^2)\hat{\Sigma}(\nabla g_{i3}(\hat{\mu}, \hat{\sigma}^2))^\top & \hat{\mu} < T. \end{cases} \quad [31]$$

Although the delta method is designed for smooth and differentiable functions, it is applicable in our context because all the functions involved are continuously differentiable. Specifically, for different samples we obtain estimators defined by functions g_1 and g_2, each corresponding to distinct scenarios, yet all satisfy the necessary smoothness conditions. For example, when $\hat{\mu} > T$, the index values are expressed as $g_{11}(\hat{\mu}, \hat{\sigma}^2)$ and $g_{21}(\hat{\mu}, \hat{\sigma}^2)$, and both functions meet the requirements for applying the delta method. Consequently, for a confidence level of $1 - \alpha$, the confidence intervals are constructed as $\hat{C}_{pni}(u,v) \pm z_{\alpha/2}\sqrt{\hat{V}_i/n}$, for $i = 1, 2$, where $z_{\alpha/2}$ denotes the critical value from the standard normal distribution.

3.2. Simulation study

A simulation is conducted to assess the performance of the proposed confidence intervals. We consider the asymmetric tolerance $(LSL, T, USL) = (20, 26, 40)$ and $u = v = 1$. Based on Eq. [31], three scenarios $\mu < T$, $\mu = T$ and $\mu > T$ are simulated. Under $\mu < T$ ($\mu > T$), we fix $\sigma = 1$ and construct 95% confidence intervals with $\mu \in [LSL, T)$ ($\mu \in (T, USL]$). For $\mu = T$, a sequence of σ involving 30 different values from 0.3 to 9 is considered. The coverage probabilities based on 10000 replications for the three scenarios are shown in Figures 4–6, where $n = 40, 80, 120, 160, 200$ are considered. As seen, the coverage probabilities are generally close to the nominal level in all the cases, and the performance improves with the sample size n. These results indicate that the proposed methods can be credibly used to construct confidence intervals of $C_{pn1}(u,v)$ and $C_{pn2}(u,v)$.

4. The non-normal case

The proposed PCIs are under the assumption that the process characteristic X follows a normal distribution. In this section, we aim to extend the proposed PCIs to the non-normal case using transformation methods. As previously discussed, one effective way involves using the inverse transformation with the CDF, offering a versatile means to convert the data into a normal distribution. Assume that X is continuous, and let $F(\cdot)$ be its CDF. It is well known that $F(X)$ follows the standard uniform distribution $U(0,1)$, and $\Phi^{-1}(F(X)) \sim N(0,1)$, where $\Phi^{-1}(\cdot)$ is the quantile function of $N(0,1)$. Consequently, our focus shifts to the estimator of $F(\cdot)$ based on the available data.

One well-known way to estimate F is to use kernel density estimation. More specifically, once the kernel density estimator $\hat{f}_h(x)$ is obtained with a suitable bandwidth h, the kernel distribution estimator is simply $\hat{F}_h(x) = \int_{-\infty}^{x} \hat{f}_h(t)dt$. This idea has been employed to construct PCIs for non-normal continuous data (Chen, Wang, and Ye 2019). Despite its widespread use, kernel density estimation is recognized for its sensitivity to the bandwidth parameter h (Eckert-Gallup and Martin 2016), influencing the smoothness of the estimators. Determining an appropriate bandwidth in practical situations is challenging, often requiring subjective judgment across diverse applications (Silverman 2018). Even if $\hat{f}_h$ proves satisfactory,

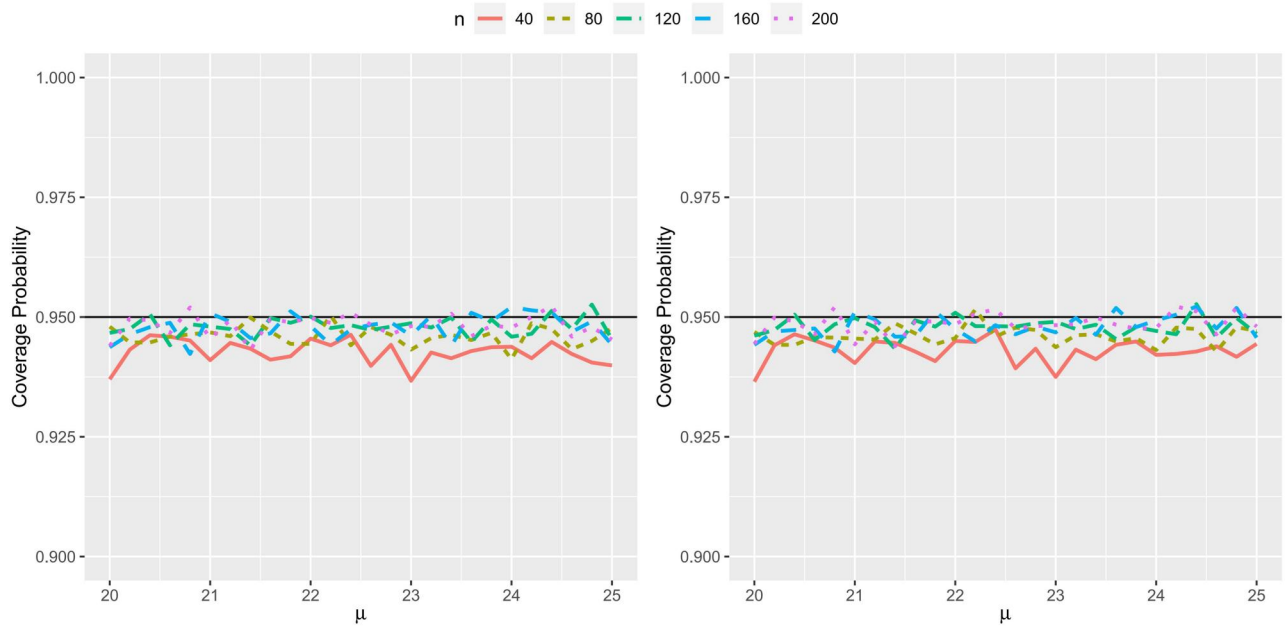

Figure 4. Coverage probabilities for 95% confidence interval with $LSL = 20$, $USL = 40$, $T = 26$, $\sigma = 1$ and different n when $\mu < T$. (left:C_{pn1}, right:C_{pn2}).

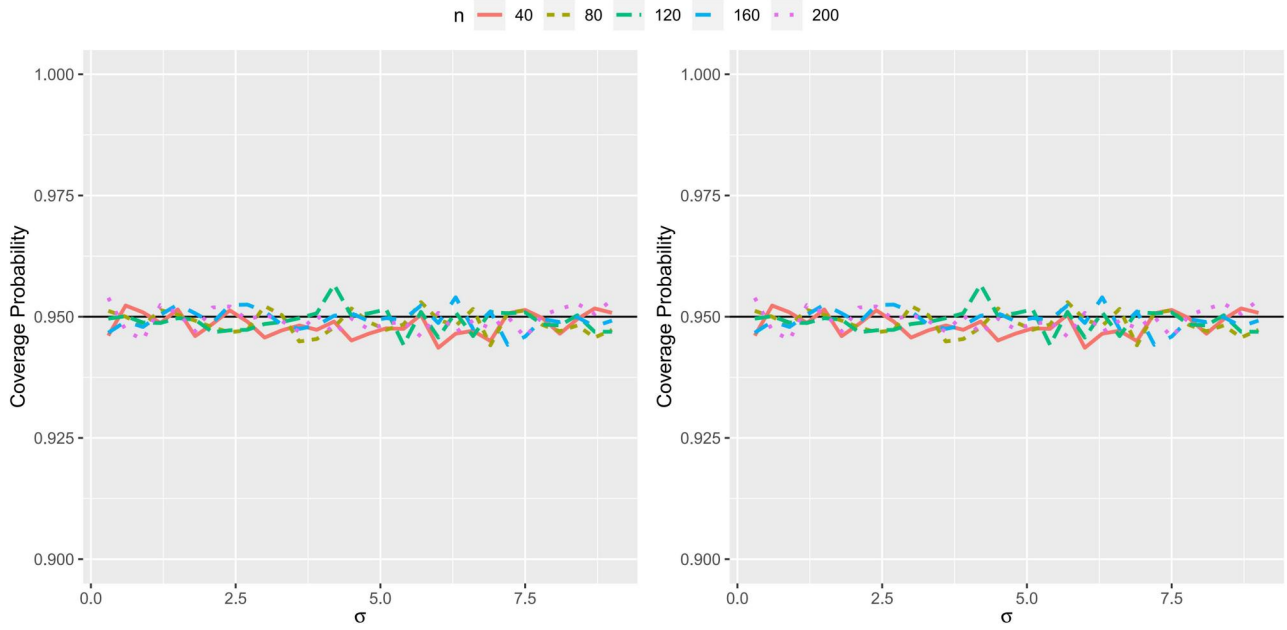

Figure 5. Coverage probabilities for 95% confidence interval with $LSL = 20$, $USL = 40$, $T = \mu = 26$ and different σ. (left:C_{pn1}, right:C_{pn2}).

the integration to obtain $\hat{F}_h$ may amplify estimation errors. Additionally, kernel estimation is not robust for the inverse transformation because it may exhibit substantial bias near the boundaries of the data range (Cheng and Peng 2002). This bias can result in invalid transformed data, as will be demonstrated later, which limits the applicability of the method proposed by Chen, Wang, and Ye (2019) for non-normal data. To overcome these shortcomings, we propose an alternative approach to estimate F using constrained B-spline regression.

4.1. The proposed method

Suppose there is a set of random samples denoted as $\boldsymbol{x} = [x_1, \ldots, x_n]^\top$, representing the quality characteristic X which is drawn from a non-normal distribution. To estimate F, a practical nonparametric approach is to

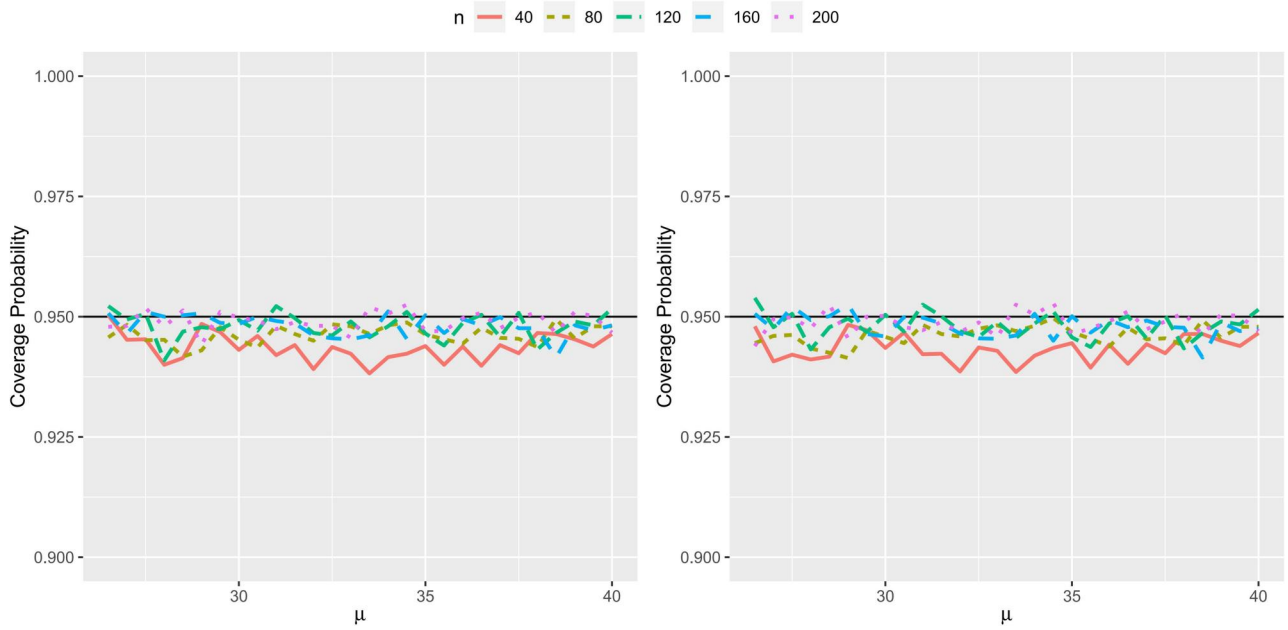

Figure 6. Coverage probabilities for 95% confidence interval with $LSL = 20$, $USL = 40$, $T = 26$, $\sigma = 1$ and different n when $\mu > T$. (left:C_{pn1}, right:C_{pn2}).

use the empirical cumulative distribution function (ECDF) denoted as $F_n(\cdot)$. Specifically, $F_n(x)$ is defined as $\sum_{i=1}^{n} I(x_i \le x)/(n+1)$ (Coles 2001), where I represents the indicator function. According to the Glivenko-Cantelli theorem, F_n converges to F with probability 1. However, it is important to note that F_n is a step function, jumping with size $1/(n+1)$ at each x_i. Directly using F_n is impractical and less accurate since F is typically continuous. To overcome this limitation, we opt for a continuous approximation of F and introduce a smooth estimator denoted as $\hat{F}_p$.

Regarding $\{F_n(x_i)\}_{i=1}^{n}$ as responses from a regression model, we have

$$F_n(x_i) = F(x_i) + \epsilon_i, \qquad i = 1, \ldots, n, \qquad [32]$$

where ϵ_i's are zero mean error terms. Such a formulation naturally motivates the use of regression techniques to estimate F and perform the inverse transformation. Xue and Wang (2010) employed spline regression due to its superior flexibility over conventional polynomial or linear approximations (Marsh and Cormier 2001). Spline functions strike an optimal balance between local adaptability and global smoothness by utilizing carefully constructed basis systems. Although various basis functions, such as I-splines (Ramsay 1988), are available, their scope is relatively limited. In contrast, B-splines (BSs) offer the significant advantage of compact local support, meaning that their nonzero values are confined to specific intervals. This localization not only improves local fitting accuracy but also enables the capture of global functional behavior through coefficient patterns. As a result, $F(x)$ can be expressed as

$$F(x) = \sum_{l=1}^{L} \beta_l B_l(x), \qquad [33]$$

where $B_l(\cdot)$ are B-splines (BSs), L is the total number of BSs and $\boldsymbol{\beta} = [\beta_1, \ldots, \beta_L]^\top$ is a vector of unknown parameters. Then, a smooth and monotone estimator of $F(\cdot)$ is produced by employing constrained regression with BSs (CBS) on n pairs $\{(x_i, F_n(x_i))\}_{i=1}^{n}$.

However, the estimator suffers from three limitations. Firstly, it relies on the least squares method, which may not be appropriate due to the heteroscedasticity in the regression model. Specifically, as indicated by the central limit theorem, the error term asymptotically follows a normal distribution, namely

$$\sqrt{n}(F_n(x) - F(x)) \xrightarrow{d} N(0, F(x)(1 - F(x))). \qquad [34]$$

Since the variance varies with x, the weighted least squares (WLS) estimation should be employed (Kantar 2015). Secondly, the estimator deviates from the desired range of [0, 1], which can result in failures during the inverse transformation, leading to infinite values. Thirdly, BSs are generally unsuitable for extrapolation. When the specification limits extend beyond the range of available samples, the estimates of $F(LSL)$ and $F(USL)$ may lack accuracy.

To address these issues and ensure reliable estimators, we propose incorporating ECDF values of the specification limits and transforming $F_n(x_i)$ before applying WLS. Instead of regarding $\{F_n(x_i)\}_{i=1}^{n}$ as

responses, we propose to use transformed pseudo-observations $y_n(x_i) = \ln[F_n(x_i)/(1 - F_n(x_i))]$, $i = 1, ..., n$, to estimate $y(x) = \ln[F(x)/(1 - F(x))]$. Due to the definition of $F_n(x)$, $y_n(x_i)$ for $i = 1, ..., n$ are always well defined. This one-to-one transformation allows us to obtain the estimated CDF $\hat{F}_p(x)$ as follows

$$\hat{F}_p(x) = \frac{e^{\hat{y}(x)}}{e^{\hat{y}(x)} + 1}, \quad [35]$$

where $\hat{y}(\cdot)$ represents a smooth estimator of $y(\cdot)$. By employing this approach, the estimate will always fall within the range of [0, 1], ensuring that $\hat{F}_p(\cdot)$ is a valid CDF estimator. Subsequently, the corresponding regression model is given by

$$y_n(x_i) = \ln\left[\frac{F_n(x_i)}{1 - F_n(x_i)}\right] = y(x_i) + \epsilon_i, \qquad i = 1, ..., n. \quad [36]$$

For simplicity, we still use ϵ_i to denote a zero mean term.

Similar as Eq. [32], we employ the BSs to approximate $y(x)$ in Eq. [36]. Defining BSs involves dividing the interval over which F is approximated into $m + 1$ subintervals using a sequence of knots or breakpoints denoted as τ_m. Specifically,

$$\tau_m = \{\min\{\boldsymbol{x}\} = s_0 < s_1 \cdots < s_{m+1} = \max\{\boldsymbol{x}\}\}. \quad [37]$$

Within each interval, polynomial functions of a specified order k (with a degree of $k - 1$) are employed to generate BSs. However, such basis functions have a limitation: they contribute only within the range of $[s_0, s_{m+1}]$ and are zero elsewhere, which becomes an issue when $LSL < s_0$ or $USL > s_{m+1}$. To overcome this, we define a new sequence over $[\min\{LSL, s_0\}, \max\{USL, s_{m+1}\}]$ instead of $[s_0, s_{m+1}]$, which is also denoted as τ_m for simplicity. Two additional corresponding transformed pseudo-observations, $y_n(LSL)$ and $y_n(USL)$, are introduced for regression. Note that $F_n(LSL)$ will be 0 if $LSL < s_0$, and hence we set it as $F_n(s_0)$ to ensure $y_n(LSL)$ will not be $-\infty$. Afterwards, estimates of $F(LSL)$ and $F(USL)$ can be obtained even if LSL and USL are beyond the range of samples.

Regarding the choice of the spline order k, Perperoglou et al. (2019) observed that for $k \geq 4$, the resulting expansions tend to be similar, with cubic B-splines (i.e., $k = 4$) being a conventional choice. Therefore, we adopt $k = 4$, which results in a total of $L = m + k$ B-spline basis functions. The parameter m is selected either to achieve the desired smoothness or based on model selection criteria, such as the AIC. Using these B-splines, the regression model is formulated as

$$y(x) = \sum_{l=1}^{L} \beta_l B_l(x).$$

We then apply WLS with the weight function defined by the variance function $G(x)$. By employing Eq. [34] and the delta method, it can be shown that the errors ϵ_i in Eq. [36] are independent and asymptotically normal with mean zero and variance $1/\{nF(x_i)[1 - F(x_i)]\}$. Consequently, the weight function is set as

$$G(x) = \frac{1}{nF_n(x)[1 - F_n(x)]},$$

where $F_n(x)$ denotes the ECDF. The variance-covariance matrix of the error term Σ_e is defined as a diagonal matrix with the principal diagonal elements given by

$$[G(x_1), ..., G(x_n), G(LSL), G(USL)]. \quad [38]$$

As previously mentioned, if $LSL < s_0$, $F_n(LSL)$ is set as $F_n(s_0)$ to prevent $-\infty$. Additionally, we enforce a non-decreasing constraint to ensure a reliable estimator, given that F, as a CDF, is inherently non-decreasing, akin to the approach in Xue and Wang (2010). Following Schumaker (2007), a sufficient condition for $\sum_{l=1}^{L} \beta_l B_l(x)$ to be non-decreasing is $\beta_{l-1} \leq \beta_l$ for $l = 2, ..., L$. Denoting $\mathcal{B}^L$ as the set of all $[\beta_1, ..., \beta_L] \in \mathcal{R}^L$ satisfying $\beta_{l-1} \leq \beta_l$, the estimates of $\boldsymbol{\beta}$ *via* WLS can be obtained by

$$\hat{\boldsymbol{\beta}} = \underset{\boldsymbol{\beta} \in \mathcal{B}^L}{\operatorname{argmin}} \sum_{i=1}^{n} \frac{(y_n(x_i) - \sum_{l=1}^{L} \beta_l B_l(x_i))^2}{G(x_i)} + \frac{(y_n(USL) - \sum_{l=1}^{L} \beta_l B_l(USL))^2}{G(USL)} + \frac{(y_n(LSL) - \sum_{l=1}^{L} \beta_l B_l(LSL))^2}{G(LSL)}. \quad [39]$$

The final smooth estimator $\hat{F}_p(\cdot)$ is then given by

$$\hat{F}_p(x) = \frac{\exp\left(\sum_{l=1}^{L} \hat{\beta}_l B_l(x)\right)}{\exp\left(\sum_{l=1}^{L} \hat{\beta}_l B_l(x)\right) + 1}. \quad [40]$$

Based on $\Phi^{-1}(\hat{F}_p(x_i))$, $i = 1, ..., n$, $\Phi^{-1}(\hat{F}_p(LSL))$, $\Phi^{-1}(\hat{F}_p(T))$ and $\Phi^{-1}(\hat{F}_p(USL))$, the estimates of two proposed PCIs can be readily obtained.

It is worth noting that Wang, Yang, and Hao (2016) also applied BSs and inverse transformation for non-normal data. Their method sought a transformation $s(\cdot)$, with a form similar to Eq. [33] and involving BSs, such that $s(X)$ follows a standard normal distribution. Specifically, they considered the relationship $q_z = s(q_x)$, where q_x and q_z denote the percentiles of the distribution F and the standard

normal distribution, respectively, with the ECDF F_n substituting for F when it is unknown. However, because $s(\cdot)$ should be non-decreasing and its range must lie within [0, 1], the lack of such constraints in their model leads to potential issues. In contrast, our method explicitly incorporates these constraints, thereby ensuring a more reliable and appropriate inverse transformation.

To analyze the efficiency of the proposed estimator, asymptotic properties are studied here. This analysis becomes particularly insightful as the sample size grows, offering a deeper understanding of the estimator's behavior and facilitating the identification of corresponding confidence regions (Van der Vaart 2000). Define $||\phi||^2 = \mathbb{E}[\phi(x)^2]$, the rate convergence, as well as the corresponding asymptotic distribution of our estimator, are shown in the following theorem and corollary. Assumptions and proofs are presented in the Supplementary Material.

Theorem 1. *Under* Assumptions (1) *to (5) in the Supplementary Material, it follows that*

$$\frac{\hat{y}(x) - y(x)}{\sigma(x)} \xrightarrow{d} N(0,1),$$

$$||\hat{y} - y|| = O_p\left(m^{-k} + \sqrt{m/n}\right),$$

where $\sigma^2(x) = \boldsymbol{B}(x)^\top (\boldsymbol{b}^\top \boldsymbol{V} \boldsymbol{b})^{-1} \boldsymbol{B}(x)$, $\boldsymbol{B}(x) = [B_1(x), ..., B_L(x)]^\top$, $\boldsymbol{b} = [\mathbf{b}_1, ..., \mathbf{b}_L]$, $\mathbf{b}_l = [B_l(x_1), ..., B_l(x_n), B_l(LSL), B_l(USL)]^\top$, *and* $\boldsymbol{V} = \Sigma_e^{-1}$. *Here,* $W_n = O_p(a_n)$ *means given a positive number* a_n

$$\lim_{c \to \infty} \limsup_n P(|W_n| \geq c a_n) = 0,$$

for all $c > 0$.

Corollary 2. *Under* Assumptions (1) *to (5) in the Supplementary Material, it follows that*

$$\frac{\hat{F}_p(x) - F(x)}{\sigma_F(x)} \xrightarrow{d} N(0,1),$$

where

$$\sigma_F^2(x) = F(x)(1 - F(x))\sigma^2(x).$$

In addition, the convergence rate of $\hat{F}_p$ *is not slower than* $\hat{y}$ *when n is sufficiently large.*

4.2. Comparison studies

In this subsection, we conduct simulation studies to assess the performance of our proposed estimator, denoted as $\hat{F}_p$. We incorporate several existing methods into our comparative studies, including kernel estimator $\hat{F}_h$, ECDF estimator $\hat{F}_e$, and the estimator based on CBS $\hat{F}_b$ (Xue and Wang 2010). Following Xue and Wang (2010), a set of knots is defined as the quantiles of artificial data. We employ m interior knots to delineate BSs during the simulation, a choice motivated by the resulting curves exhibiting a satisfactory smoothness when observed in transformed pseudo-observations. Consequently, the knots correspond to the $1/(m+1), 2/(m+1), ..., m/(m+1)$ quantiles of the data.

We assume that X follows one of three distributions that are commonly used to model process data (Ryan 2011): the Weibull distribution $WB(k, 1)$ (with shape parameter k and scale 1), the log-normal distribution $LN(\mu, 1)$ (with location parameter μ and scale 1), and the gamma distribution $GA(\theta, 2)$ (with shape parameter θ and rate 2). Additional parameter settings are considered in the Supplementary Material. The upper and lower specification limits (USL and LSL) are set as the 0.99 and 0.01 quantiles of the true distribution, respectively, and the target value is defined as $T = M = (LSL + USL)/2$. As a result, the inverse transformation leads to asymmetric tolerances. Taking C_{pn1} as an example, for a given sample vector $\boldsymbol{x} = [x_1, ..., x_n]^\top$ generated from a specified distribution with fixed parameters, we compute the corresponding index values based on the estimated CDF, denoted as $\hat{C}_{pn1}^h$, $\hat{C}_{pn1}^e$, $\hat{C}_{pn1}^b$, and $\hat{C}_{pn1}^p$. This simulation is repeated 1000 times. We evaluate the performance of various estimators using two types of log mean squared error (LMSE), defined as

$$\begin{aligned} \text{LMSE}_{\text{CDF}} &= \frac{1}{1000} \sum_{j=1}^{1000} \log_{10} \left[\frac{1}{n} \sum_{i=1}^{n} \left(\hat{F}(x_i^{(j)}) - F(x_i^{(j)}) \right)^2 \right], \\ \text{LMSE}_{\text{PCI}} &= \frac{1}{1000} \sum_{j=1}^{1000} \log_{10} \left[\left(\hat{C}_{pn1}^{(j)} - C_{pn1}^{(j)} \right)^2 \right], \end{aligned} \tag{41}$$

where the superscript (j) denotes the value obtained in the jth replication. Here, $\hat{F}(\cdot)$ is the estimate of the true CDF $F(\cdot)$, and $\hat{C}_{pn1}$ and C_{pn1} represent the estimated and true PCI values, respectively.

We first assess the performance of our CDF estimator. For this experiment, we set $k = 1$, $\mu = 0$, and $\theta = 1$, and consider 20 different sample size n ranging from 50 to 1000. Additional simulation settings and results are provided in the Supplementary Material. Figure 7 illustrates the average LMSE_{CDF}, where our method outperforms all other approaches. This superior performance is attributable to two main factors. First, our estimation directly targets the CDF, thereby avoiding the extra error introduced by the integral calculation required in kernel estimators. Second, our

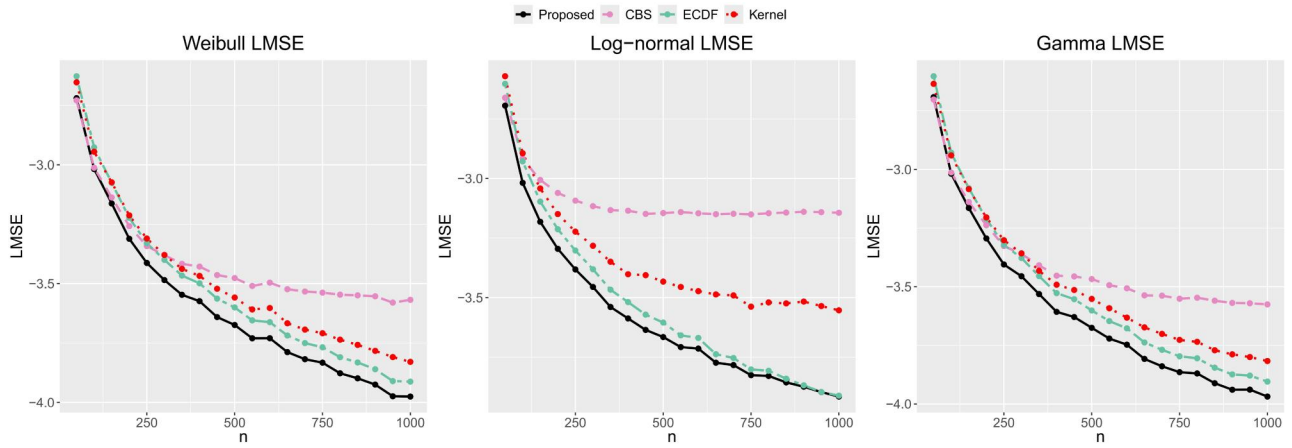

Figure 7. The average LMSE_{CDF} of different methods based on 20 different sample sizes $n \in \{50, 100, \ldots, 1000\}$ for $WB(1,1)$, $LN(0,1)$ and $GA(1,2)$.

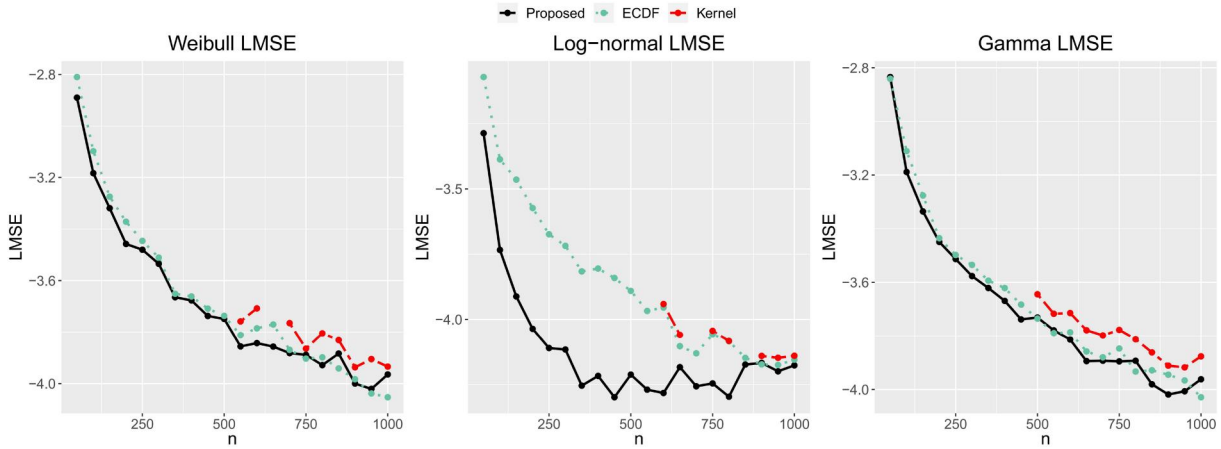

Figure 8. The average LMSE_{PCI} of different methods based on 20 different sample sizes $n \in \{50, 100, \ldots, 1000\}$ for $WB(1,1)$, $LN(0,1)$ and $GA(1,2)$.

use of transformed pseudo-observations offers a clear advantage over the CBS-based estimator. In particular, the CBS-based estimator $\hat{F}_b$ sometimes produces estimates outside the valid range of [0, 1], leading to higher LMSE values. In contrast, our proposed estimator consistently guarantees that the estimated CDF remains within the proper range. Furthermore, although both $\hat{F}_p$ and $\hat{F}_e$ are based on the ECDF, our method employs a WLS approach to yield a continuous estimator. This refinement results in higher accuracy compared to directly using the ECDF, as evidenced by the lower LMSE values achieved by our estimator.

We then evaluate the performance of the PCI estimators, with the results illustrated in Figure 8. Notably, $\hat{C}^b_{pn1}$ encounters significant issues across all three distributions considered. Since CBS is insensitive to the range of the CDF, its application results in infinite values after the data transformation, making it impractical for PCI calculations. This problem is especially pronounced for the gamma distribution $GA(1,2)$, as detailed in Table 2, where CBS fails in the majority of replications across various sample sizes n. These findings underscore the importance of employing transformed pseudo-observations in our proposed method. Consequently, for LMSE evaluation we focus on $\hat{C}^h_{pn1}$, $\hat{C}^e_{pn1}$, and $\hat{C}^p_{pn1}$. In particular, $\hat{C}^h_{pn1}$ exhibits some missing points, suggesting limitations with small sample sizes—especially when the USL exceeds the sample range, leading to $\hat{F}_k(USL) = 1$ and the transformed USL becoming $+\infty$, which makes it unsuitable for evaluation. In contrast, our proposed estimator $\hat{C}^p_{pn1}$ demonstrates robustness, with estimates based on Eq. [40] consistently falling within the valid range of [0, 1]. Furthermore, the results indicate that our method provides reliable estimates at specification limits, even when these limits extend beyond the range of the available data.

Table 2. Percentage of failures in calculating PCI values using $\hat{F}_b$ for $GA(1,2)$ across different sample sizes.

n	50	100	150	200	250	300	350	400	450	500
Percentage	38.3%	62.4%	71.4%	79.6%	85.1%	86.6%	92.1%	94.1%	96.1%	97.9%
n	550	600	650	700	750	800	850	900	950	1000
Percentage	98.3%	98.2%	99.2%	98.7%	99.2%	99.8%	100%	99.9%	99.6%	100%

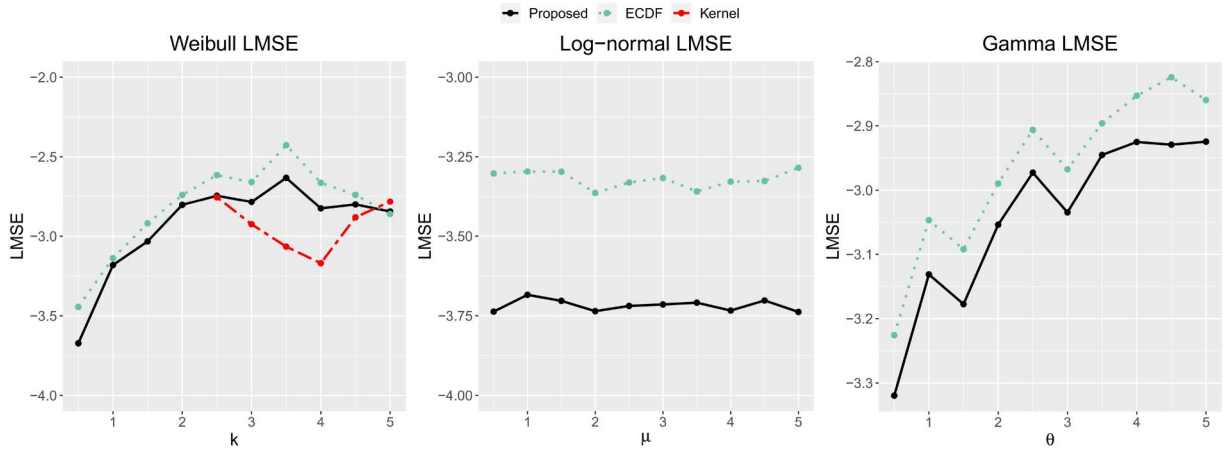

Figure 9. The average LMSE_{PCI} based on different methods for $WB(k,1)$, $LN(\mu,1)$ and $GA(\theta,2)$ with different parameters ranging from 0.5 to 5 and the same sample size of 100.

Table 3. Percentage of failures using $\hat{F}_k$ and $\hat{F}_b$ to calculate PCI values for $GA(\theta,2)$ with $n = 100$.

θ	0.5	1	1.5	2	2.5	3	3.5	4	4.5	5
Kernel	25.9%	13.3%	10.3%	5.6%	3.6%	2.2%	1.1%	1.4%	0.7%	0.7%
CBS	25.4%	26.9%	22.9%	22.7%	22.4%	20.6%	23.6%	24.1%	20.4%	21.7%

Furthermore, we fix the sample size at $n = 100$ and evaluate the performance under varying parameter values by setting k, μ, and θ to $0.5, 1, \ldots, 5$. Additional simulation settings and results are provided in the Supplementary Material. Here, we focus exclusively on comparing the four methods in terms of PCI values. Figure 9 presents the LMSEs based on PCI values for all methods except CBS, demonstrating that our proposed method generally outperforms the other two approaches. Similar to CBS, the kernel estimation method also struggles with the inverse transformation. For instance, Table 3 reports the percentage of failures in calculating PCIs over 1000 replications for different values of θ in the $GA(\theta,2)$ distribution. The underlying reasons for these failures differ between the two methods. The kernel estimator is particularly prone to failure when the sample size is small or the distribution exhibits a heavy tail. In such cases, the specification limits often fall outside the observed data range, leading to estimated CDF values of 0 or 1. In contrast, CBS-based estimation becomes increasingly problematic as the sample size grows, with the failure rate of $\hat{F}_b$ rising accordingly. In comparison, our proposed method incorporates transformed pseudo-observations and constructs a new sequence of knots that explicitly includes the specification limits. These features enhance its suitability for the inverse transformation, ensuring more reliable PCI estimation across different parameter settings.

5. Illustrative example

In this section, we apply the proposed two PCIs along with the normalized method to a real dataset of non-polarized capacitors obtained from an electronics company. These capacitors are utilized in high-fidelity audio speaker systems for high-pitch, mid-pitch, and low-pitch crossover networks. The manufacturing process encompasses a series of meticulous steps, beginning with the precision cutting of aluminum foil rolls into slender strips. Subsequent stages involve thorough cleaning, the expert stitching of lead wire, and the meticulous formation of the capacitor's interior by carefully rolling paper and sheets of aluminum foil. This is followed by the assembly of an aluminum case, the application of a rubber end seal, the addition of a PVC sleeve, and the immersion of the capacitor's interior in an electrolytic solution. Finally, the product undergoes a crucial aging process to ensure its optimal performance. We regard the capacitance of the

Table 4. Capacitances (in μF) of non-polarized capacitors from two different processes.

P_1	292	293	294	294	294	294	294	294	295	295	295	295	295	295	295
	296	296	296	297	297	297	297	297	298	298	298	298	298	298	298
	299	299	299	300	300	300	300	300	301	301	301	301	302	302	302
	302	302	302	302	303	303	303	303	303	303	304	304	304	304	304
	305	305	305	305	305	305	306	306	306	306	306	306	307	307	307
	308	308	308	308	309	309	309	309	309	309	310	310	310	311	312
	312	313	313	313	313	315	316	319	320	324					
P_2	291	291	292	293	293	294	294	294	294	294	294	295	295	295	295
	295	295	296	296	296	296	296	296	296	296	296	297	297	297	297
	297	297	297	297	297	297	298	298	298	298	298	298	298	298	298
	298	298	298	298	299	299	299	299	299	299	299	299	299	300	300
	300	300	300	300	300	300	301	301	301	301	301	301	301	301	302
	302	302	302	302	302	302	302	303	303	303	303	304	304	304	304
	304	304	305	305	305	306	307	307	310	313					

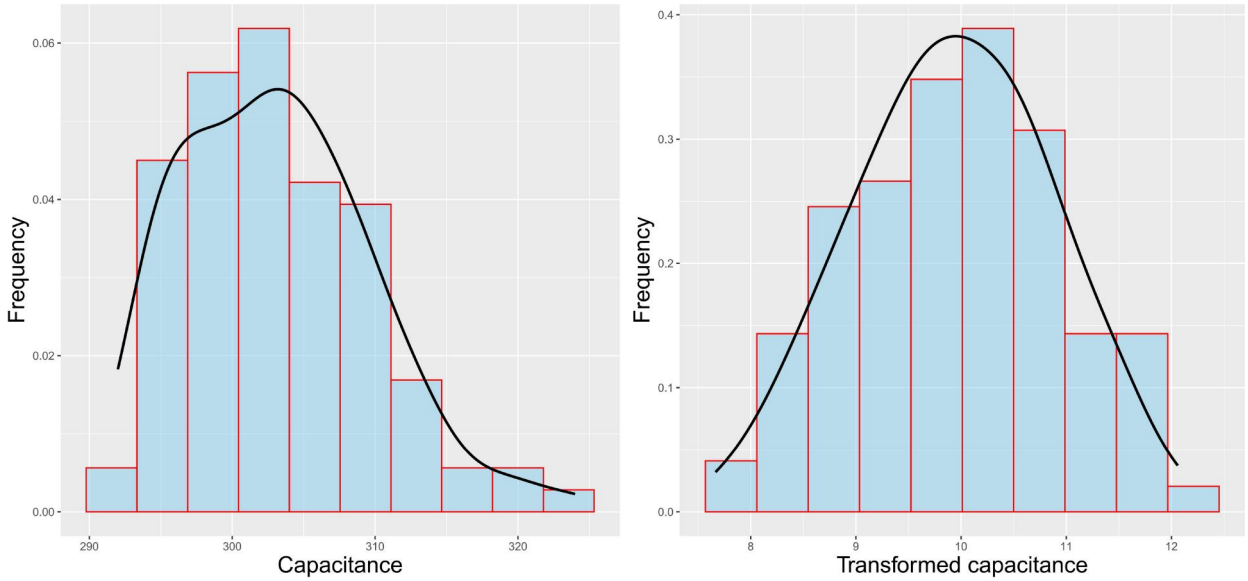

Figure 10. Histograms of original samples from P_1 (left) and transformed samples (right).

capacitor as its quality characteristic, which can be any value between 1 μF and 1000 μF, according to Pearn and Chen (1997). For a particular type of aluminum non-polarized capacitor, the upper and lower specification limits of the capacitance specified by the customers are 285 and 315 (in μF), respectively. The target value is the midpoint between the two specification limits, which is 300 μF. A total of 200 samples of non-polarized capacitors from two different processes are presented in Table 4.

We commence our analysis by examining the data from the first production process denoted as P_1. The left histogram in Figure 10 shows that the original samples follow a skewed distribution, which motivates the use of the transformation method. We start by computing the ECDF from the data of process P_1. The transformed pseudo-observations, defined in Eq. [36], are then used as the responses in the spline regression model. Consistent with our comparison study, knots are selected at the $1/16, \ldots, 15/16$ quantiles of the P_1 data to construct the BS basis functions. The WLS approach, as described in Eq. [39], is used to estimate the coefficients $\hat{\boldsymbol{\beta}}$. The corresponding estimated CDF, $\hat{F}_p$, given in Eq. [40] and shown in Figure 11, closely aligns with the ECDF points, capturing the overall trend effectively. Finally, the data from P_1 is transformed using $\Phi^{-1}(\hat{F}_p(\cdot))$ to achieve normality.

The right panel of Figure 10 suggests that the transformed data approximately follows a normal distribution. To further verify normality, we perform a Shapiro-Wilk test, obtaining $p = 0.009553$ before transformation and $p = 0.7458$ afterward. The sufficiently large p-value post-transformation confirms that the transformed data conforms to a normal distribution. Subsequently, the new specification limits LSL, T, and USL are determined as 7.65, 9.61, and 12.22, respectively, indicating that the new target is not centered between the new limits. Therefore, we apply the proposed PCI measures to evaluate process P_1.

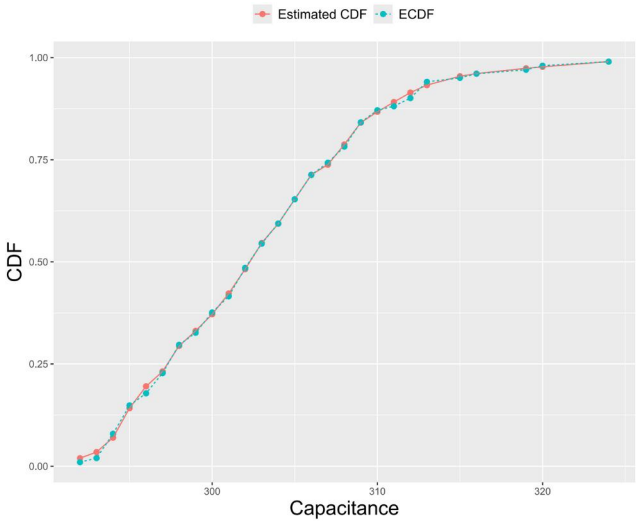

Figure 11. Estimated CDF *via* the proposed method and the ECDF based on data from P_1.

Table 5. Points estimates and 95% confidence intervals of two proposed PCIs, along with the corresponding upper bounds of non-conforming (NC) percentage.

	PCIs	Estimate	95% confidence interval	Upper bound of NC
P_1	C_{pn1}	0.5311	[0.4158, 0.6465]	32.47%
	C_{pn2}	0.5181	[0.4013, 0.6350]	35.34%
P_2	C_{pn1}	0.5953	[0.5050, 0.6856]	23.82%
	C_{pn2}	0.5727	[0.4744, 0.6709]	30.73%

Similarly, we transform 100 observations from the second process, P_2, leading to asymmetric tolerances. The Shapiro-Wilk test yields a p-value of 0.046 before transformation, which increases to 0.5132 afterward, further supporting the normality assumption post-transformation.

The results of applying the proposed PCIs to the two processes are summarized in Table 5. These findings indicate minimal differences between the two PCI measures, both consistently suggesting that the second process exhibits higher quality. It is worth noting that the upper bound of NC tends to be conservative, as illustrated in Figure 3. As a result, the upper bounds of NC based on our PCIs are relatively high for both processes. Nevertheless, the lower values of P_2 further support its superior performance. As highlighted by Pearn and Chen (1997), after sampling from P_1, several process improvements, including Taguchi's parameter designs, were implemented to enhance overall manufacturing quality. A subsequent set of 100 samples was then collected from the refined process, P_2. The improved performance of P_2 aligns with the conclusions drawn from the proposed PCIs. In summary, our proposed PCIs, along with the normalized method, effectively account for both non-normal data and asymmetric tolerances. These indices serve as valuable tools for evaluating production processes and capturing improvements in quality.

6. Conclusion

In this study, we tackled two critical challenges in process capability analysis: accommodating asymmetric tolerances and non-normal quality characteristics. Unlike most existing studies that address these issues separately, our work integrates both aspects to offer a comprehensive evaluation framework for manufacturing processes. We began by reviewing the essential properties of PCIs under asymmetric tolerances in normally distributed settings and found that no existing PCI satisfies all the desired properties. To bridge this gap, we introduced two novel classes of PCIs, complete with parametric estimation procedures and asymptotic confidence limits. Our comparative analysis with existing methods highlighted the advantages of our approach, particularly in terms of effectively capturing process centering and yield. Recognizing the prevalence of non-normal data in practical applications, we extended our methodology by employing constrained B-spline regression on transformed pseudo-observations to accurately estimate the CDF. In addition, we developed a tailored inverse transformation to normalize the data, which proved essential for reliable PCI estimation under non-normal conditions. Simulation studies confirmed the superiority of our approach across various scenarios. Finally, we applied the proposed PCIs and transformation method to a real manufacturing data set, demonstrating their practical applicability and robustness. In conclusion, our unified framework successfully addresses the challenges of asymmetric tolerances and non-normal data simultaneously, providing a valuable tool for comprehensive process capability assessment in diverse manufacturing environments.

About the authors

Shixiang Li received his bachelor's degree in Statistics from Beijing Institute of Technology in 2018. He is currently pursuing his Ph.D. degree at the Delft University of Technology. His research interests focus on experimental design and reliability engineering.

Sheng Fu is an Associate Professor at Nankai University. Prior to this position, he completed a Postdoctoral training at both the National Institutes of Health and the National University of Singapore. He obtained his Ph.D. degree from the University of Chinese Academy of Sciences, where he also completed a year of joint Ph.D. training at the University of North Carolina at Chapel Hill. His research interests include biostatistics and machine learning.

Dianpeng Wang received his bachelor's degree in 2007, master's degree in 2010, and Ph.D. degree in 2016, all from Beijing Institute of Technology. He is currently an Associate Professor at the School of Mathematics and Statistics, Beijing Institute of Technology. His research interests include computer experiment design, Bayesian calculation, uncertainty quantification, and industrial big data analysis.

Piao Chen is an Associate Professor at the ZJUI Institute, Zhejiang University. Prior to this position, he served as an assistant professor in statistics at TU Delft from 2020 to 2023. He obtained a Bachelor's degree in Industrial Engineering from Shanghai Jiao Tong University in 2013 and a Ph.D. in Industrial Systems Engineering and Management from the National University of Singapore in 2017. His research primarily focuses on quality and reliability, statistical learning, and operations research.

Acknowledgment

We are grateful to the editor and anonymous referees for their insightful comments, which have led to substantial improvements to an earlier version of this paper. We also thank Professor Geurt Jongbloed for his valuable discussions and comments.

Disclosure statement

No potential conflict of interest was reported by the authors.

Funding

This work was supported in part by the National Natural Science Foundation of China under Grant 72401253, Grant 12131001, and Grant 12171033, in part by the State Key Laboratory of Biobased Transportation Fuel Technology under Grant 512302-X02301, and in part by the Fundamental Research Funds for the Central Universities (054-63253111) and Tianjin Municipal S&T Grant (24JCQNJC02000).

Data availability statement

The data that support the findings of this study are openly available in Pearn and Chen (1997).

References

Abbasi Ganji, Z., and B. Sadeghpour Gildeh. 2016. A class of process capability indices for asymmetric tolerances. *Quality Engineering* 28 (4):441–54. doi: 10.1080/08982112.2016.1168524.

Bittanti, S., M. Lovera, and L. Moiraghi. 1998. Application of non-normal process capability indices to semiconductor quality control. *IEEE Transactions on Semiconductor Manufacturing* 11 (2):296–303. doi: 10.1109/66.670179.

Boyles, R. A. 1994. Brocess capability with asymmetric tolerances. *Communications in Statistics - Simulation and Computation* 23 (3):615–35. doi: 10.1080/03610919408813190.

Chen, K., and W. Pearn. 1997. An application of non-normal process capability indices. *Quality and Reliability Engineering International* 13 (6):355–60. doi: 10.1002/(SICI)1099-1638(199711/12)13:6<355::AID-QRE125>3.0.CO;2-V.

Chen, K.-S., and W.-L. Pearn. 2001. Capability indices for processes with asymmetric tolerances. *Journal of the Chinese Institute of Engineers* 24 (5):559–68. doi: 10.1080/02533839.2001.9670652.

Chen, P., B. X. Wang, and Z.-S. Ye. 2019. Yield-based process capability indices for nonnormal continuous data. *Journal of Quality Technology* 51 (2):171–80. doi: 10.1080/00224065.2019.1571342.

Cheng, M.-Y, and L. Peng. 2002. Regression modeling for nonparametric estimation of distribution and quantile functions. *Statistica Sinica* 12 (4):1043–60.

Clements, J. A. 1989. Process capability calculations for non-normal distributions. *Quality Progress* 22:95–100.

Coles, S. 2001. *An introduction to statistical modeling of extreme values*. London: Springer.

Cui, Y., J. Yang, and S. Huang. 2018. Interval estimation of process capability indices based on the quality data of supplied products. In *2018 12th International Conference on Reliability, Maintainability, and Safety (ICRMS)*, 400–4.

Dariae, D., and B. Sadeghpour Gildeh. 2017. Capability indices for Rayleigh process. *Journal of System Management* 3 (2):61–76.

de Almeida, M. H., P. L. Ramos, G. S. Rao, and F. A. Moala. 2021. Objective Bayesian inference for the capability index of the Gamma distribution. *Quality and Reliability Engineering International* 37 (5):2235–47. doi: 10.1002/qre.2854.

Dey, S., M. Saha, M. Anis, S. S. Maiti, and S. Kumar. 2023. Estimation and confidence intervals of CNp (u, v) for logistic-exponential distribution with application. *International Journal of System Assurance Engineering and Management* 14 (Suppl 1):431–46. doi: 10.1007/s13198-023-01870-y.

Eckert-Gallup, A., and N. Martin. 2016. Kernel density estimation (KDE) with adaptive bandwidth selection for environmental contours of extreme sea states. In OCEANS 2016 MTS/IEEE Monterey, 1–5.

Erfanian, M., and B. Sadeghpour Gildeh. 2021. A new capability index for non-normal distributions based on linex loss function. *Quality Engineering* 33 (1):76–84. doi: 10.1080/08982112.2020.1761026.

Franklin, L. A., and G. S. Wasserman. 1992. Bootstrap lower confidence limits for capability indices. *Journal of Quality Technology* 24 (4):196–210. doi: 10.1080/00224065.1992.11979401.

Grau, D. 2005. Algebraic relationship between symmetrical and asymmetrical capability indices. *Quality Engineering* 17 (3):359–70. doi: 10.1081/QEN-200062247.

Guo, B., Q. Xia, Y. Sun, and M. Aslam. 2023. Generalized confidence intervals of quantile-based process capability indices for inverse Gaussian distribution. *Quality*

Technology & Quantitative Management 20 (3):405–17. doi: 10.1080/16843703.2022.2126260.
Kane, V. E. 1986. Process capability indices. *Journal of Quality Technology* 18 (1):41–52. doi: 10.1080/00224065.1986.11978984.
Kantar, Y. M. 2015. Generalized least squares and weighted least squares estimation methods for distributional parameters. *REVSTAT-Statistical Journal* 13 (3):263–82.
Kashif, M., S. Ullah, M. Aslam, and M. Z. Iqbal. 2023. Robust process capability indices Cpm and Cpmk using Weibull process. *Scientific Reports* 13 (1):16977. doi: 10.1038/s41598-023-44267-4.
Khlil, S., H. Al-Khazraji, and Z. Alabacy. 2020. Process capability analysis to assess capacity of a cleaning liquid product with asymmetric tolerances. *Engineering and Technology Journal* 38 (6):910–6. doi: 10.30684/etj.v38i6A.905.
Kumar, S., A. S. Yadav, S. Dey, and M. Saha. 2022. Parametric inference of generalized process capability index Cpyk for the power Lindley distribution. *Quality Technology & Quantitative Management* 19 (2):153–86. doi: 10.1080/16843703.2021.1944966.
Kushler, R. H., and P. Hurley. 1992. Confidence bounds for capability indices. *Journal of Quality Technology* 24 (4):188–95. doi: 10.1080/00224065.1992.11979400.
Marsh, L. C., and D. R. Cormier. 2001. *Spline regression models*. Thousand Oaks, CA: Sage.
Momeni, F., B. Sadeghpour Gildeh, and G. Hesamian. 2019. Fuzzy nonparametric estimation of capability index C_{pk}. *Soft Computing* 23 (20):10485–94. doi: 10.1007/s00500-018-3614-y.
Oehlert, G. W. 1992. A note on the delta method. *The American Statistician* 46 (1):27–9. doi: 10.1080/00031305.1992.10475842.
Otsuka, A., and F. Nagata. 2018. Quality design method using process capability index based on Monte-Carlo method and real-coded genetic algorithm. *International Journal of Production Economics* 204:358–64. doi: 10.1016/j.ijpe.2018.08.016.
Ouyang, L., S. Dey, and C. Park. 2024. Robust confidence intervals for the process capability index Cpk with bootstrap improvement. *Quality Engineering* 36 (3):624–37. doi: 10.1080/08982112.2023.2263523.
Parchami, A., and M. Mashinchi. 2007. Fuzzy estimation for process capability indices. *Information Sciences* 177 (6):1452–62. doi: 10.1016/j.ins.2006.08.016.
Pearn, W., and K. Chen. 1997. Capability indices for non-normal distributions with an application in electrolytic capacitor manufacturing. *Microelectronics Reliability* 37 (12):1853–8. doi: 10.1016/S0026-2714(97)00023-1.
Perperoglou, A., W. Sauerbrei, M. Abrahamowicz, and M. Schmid. 2019. A review of spline function procedures in R. *BMC Medical Research Methodology* 19 (1):46. doi: 10.1186/s12874-019-0666-3.
Ramsay, J. O. 1988. Monotone regression splines in action. *Statistical Science* 3 (4):425–41. doi: 10.1214/ss/1177012761.
Riani, M., A. C. Atkinson, and A. Corbellini. 2023. Automatic robust Box–Cox and extended Yeo–Johnson transformations in regression. *Statistical Methods & Applications* 32 (1):75–102. doi: 10.1007/s10260-022-00640-7.
Rosas Rivera, L. A., N. F. Hubele, and F. P. Lawrence. 1995. Cpk index estimation using data transformation. *Computers & Industrial Engineering* 29 (1-4):55–8. doi: 10.1016/0360-8352(95)00045-3.
Ryan, T. P. 2011. *Statistical methods for quality improvement*. Hoboken, NJ: John Wiley & Sons.
Schumaker, L. 2007. *Spline functions: Basic theory*. New York: Cambridge University Press.
Senvar, O., and C. Kahraman. 2014. Type-2 fuzzy process capability indices for non-normal processes. *Journal of Intelligent & Fuzzy Systems* 27 (2):769–81. doi: 10.3233/IFS-131035.
Shaabani, J., and A. Jafari. 2024. Inference on the lifetime performance index of gamma distribution: Point and interval estimation. *Communications in Statistics - Simulation and Computation* 53 (3):1368–86. doi: 10.1080/03610918.2022.2045498.
Silverman, B. 2018. *Density estimation for statistics and data analysis*. New York: Routledge.
Tang, L. C., and S. E. Than. 1999. Computing process capability indices for non-normal data: A review and comparative study. *Quality and Reliability Engineering International* 15 (5):339–53. doi: 10.1002/(SICI)1099-1638(199909/10)15:5<339::AID-QRE259>3.0.CO;2-A.
Tomohiro, R., I. Arizono, and Y. Takemoto. 2020. Economic design of double sampling Cpm control chart for monitoring process capability. *International Journal of Production Economics* 221:107468. doi: 10.1016/j.ijpe.2019.08.003.
Van der Vaart, A. W. 2000. *Asymptotic statistics*. New York: Cambridge University Press.
Vännman, K. 1995. A unified approach to capability indices. *Statistica Sinica* 5 (2):805–20.
Vännman, K. 1997. A general class of capability indices in the case of asymmetric tolerances. *Communications in Statistics - Theory and Methods* 26 (8):2049–72. doi: 10.1080/03610929708832031.
Wang, C.-H., and K.-S. Chen. 2020. New process yield index of asymmetric tolerances for bootstrap method and six sigma approach. *International Journal of Production Economics* 219:216–23. doi: 10.1016/j.ijpe.2019.05.004.
Wang, C.-H., K.-S. Chen, and K.-H. Tan. 2019. Lean six sigma applied to process performance and improvement model for the development of electric scooter water-cooling green motor assembly. *Production Planning & Control* 30 (5–6):400–12. doi: 10.1080/09537287.2018.1501810.
Wang, H., J. Yang, and S. Hao. 2016. Two inverse normalizing transformation methods for the process capability analysis of non-normal process data. *Computers & Industrial Engineering* 102:88–98. doi: 10.1016/j.cie.2016.10.014.
Wang, S., J.-Y. Chiang, T.-R. Tsai, and Y. Qin. 2021. Robust process capability indices and statistical inference based on model selection. *Computers & Industrial Engineering* 156:107265. doi: 10.1016/j.cie.2021.107265.
West, R. M. 2022. Best practice in statistics: The use of log transformation. *Annals of Clinical Biochemistry* 59 (3):162–5. doi: 10.1177/00045632211050531.
Wu, C.-W., M.-H. Shu, W. L. Pearn, and Y.-C. Tai. 2010. Estimating and testing process accuracy with extension to

asymmetric tolerances. *Quality & Quantity* 44 (5):985–95. doi: 10.1007/s11135-009-9243-x.

Wu, C.-W., W. Pearn, and S. Kotz. 2009. An overview of theory and practice on process capability indices for quality assurance. *International Journal of Production Economics* 117 (2):338–59. doi: 10.1016/j.ijpe.2008.11.008.

Xue, L., and J. Wang. 2010. Distribution function estimation by constrained polynomial spline regression. *Journal of Nonparametric Statistics* 22 (4):443–57. doi: 10.1080/10485250903336802.

Zou, Z., Q. Wang, Q. Wu, M. Li, J. Zhen, D. Yuan, M. Zhou, C. Xu, Y. Wang, Y. Zhao, et al. 2024. Inversion of heavy metal content in soil using hyperspectral characteristic bands-based machine learning method. *Journal of Environmental Management* 355:120503. doi: 10.1016/j.jenvman.2024.120503.